

# EXHIBIT K



**ESi**

# **Rebuttal to Plaintiff's Expert Report**

**UNKNOWN PLS V. CHART, INC. ET AL**

SAN FRANCISCO, CALIFORNIA

ESi File No.: 70497H

ESi Descriptor: Unknown Pls V. Chart, Inc., et al.

Your Client: Chart, Inc.

Claim No.: 3:18-cv-01586-JSC

Date of Loss: March 4, 2018



2355 Polaris Ave N  
Plymouth, MN 55447

# Rebuttal to Plaintiff's Expert Report

## UNKNOWN PLS V. CHART, INC. ET AL

ESI Project No: 70497H

**Report Prepared For:**

Mr. Kevin M. Ringel  
Swanson, Martin, & Bell, LLP  
330 N. Wabash, Suite 3300  
Chicago, IL 60611

**Submitted by:**

A handwritten signature in black ink that reads "RJ Parrington".

---

December 4, 2020

Date

**Ronald J. Parrington, P.E., FASM**  
**Senior Managing Consultant**  
**NY P.E. | Expires: August 31, 2021**

**Technical Review by:**

A handwritten signature in black ink that reads "Jeffrey L. McDougall".

---

December 4, 2020

Date

**Jeffrey L. McDougall, P.E.**  
**Senior Consultant**  
**GA P.E. | Expires December 31, 2020**

This report and its contents are the Work Product of Engineering Systems Inc. (ESI). This report should only be duplicated or distributed in its entirety. This report may contain confidential or court protected information; please contact an authorized entity prior to distributing. Conclusions reached and opinions offered in this report are based upon the data and information available to ESI at the time of this report and may be subject to revision after the date of publication, as additional information or data becomes available.

Copyright ESI © 2020 - All Rights Reserved



## Background

---

Engineering Systems Inc. (ESI) was retained by Swanson, Martin, & Bell, LLP on behalf of Chart Industries, Inc. ("Chart") to perform an investigation related to a loss of liquid nitrogen in a cryogenic storage tank at Pacific Fertility Center in San Francisco, California on March 4, 2018 (the "Incident"). The Incident involved a Chart-manufactured MVE 808AF-GB Cryogenic Freezer known as "Tank 4."

The results of ESI's metallurgical investigation into this matter were provided in an expert report dated 6-November-2020. The purpose of this report is to address claims made by Plaintiff's expert, Dr. Anand Kasbekar, in his report dated 6-November-2020, and in his deposition taken on 25-November-2020. My rate is \$375 per hour. Dr. Jay Sohn, who performed the finite element analysis presented in Appendix 1 to this report, has an hourly rate of \$285. Payment is not contingent upon the outcome of the case.

## Basis for this Report

---

This report, and the opinions and conclusions stated throughout, are based on the education, training, and experience of the author, as well as on the analysis and review of materials that have been conducted in this matter to date. The opinions and conclusions are stated to a reasonable degree of engineering and scientific certainty.

A listing of the materials reviewed as part of my investigation and analysis are included in Addendum C to my expert report dated 6-November-2020. My curriculum vitae (CV), which includes my professional qualifications and a list of publications, is included in Addendum D to my expert report dated 6-November-2020. Below is a list of materials that were relied upon for my investigation to date.

- Inspection Documents, September 6, 2019:
  - Field Notes of Ronald J. Parrington, P.E., FASM
- Inspection Documents, March 11-13, 2020
  - Inspection Notes of Ronald J. Parrington, P.E.
  - Tank Inspection Materials/Data
  - 5005-8541 Exponent – Chemical Testing Results
- Non-ESI Testing (Exponent) continued Metallography-Microhardness Inspection August 24, 2020:
  - Metallography
  - Microhardness
  - Supplemental Photographs
  - Inspection Protocol (Exponent)
- Laser Scan Screenshots taken by Christopher J. Brand, P.E., 08-14-2019
- Photographs taken by Christopher J. Brand, P.E., 09-06-2019
- Photographs taken by Ronald J. Parrington, P.E., FASM, 09-06-2019



- Photographs taken by Christopher J. Brand, P.E., 09-30-2019
- Photographs taken by Christopher J. Brand, P.E., 10-01-2019
- Photographs taken by Christopher J. Brand, P.E., 03-11-2020 – 03-13-2020
- Photographs taken by Ronald J. Parrington, P.E., FASM, 03-11-2020 – 03-13-2020
- Proposed Tank and Controller Testing Protocol (ID 710846)
- Chart Drawings (PROD003)
  - CHART000115
  - CHART070445
- Exponent – Metallurgical Mount Sectioning Proposal, July 2, 2020
- Keyence Images from Exponent
- Reference Materials:
  - Tanzer, A., "Determination and Classification of Damage", ASM Handbook, Volume 11, Failure Analysis and Prevention, 2002, P. 345, Table 1.
  - Nishimura, A. and Mukai, Y., "Cold Thermal Fatigue of Austenitic Stainless Steel", Advances in Cryogenic Engineering (Materials), Vol. 38, Edited by F.R. Fickett and R.P. Reed, Plenum Press, New York, 1992.
  - I.K. Heo, D.H. Yoon, J.H. Kim, H.C. Kim, K.D. Kim, "Fatigue crack propagation behavior in AISI 304 steel welded joints for cold-stretched liquefied natural gas (LNG) storage tank at cryogenic temperatures", Materialwiss. Werkstofftech. 2019, 50, 580–587.
  - ASM Handbook, Volume 11, Failure Analysis and Prevention, 2002, P. 1069.
  - Kenichi Suzuki, Juichi Fukakura, and Hideo Kashiwaya, "Cryogenic Fatigue Properties of 304L and 316L Stainless Steels Compared to Mechanical Strength and Increasing Magnetic Permeability", Journal of Testing and Evaluation, JTEVA, Vol. 16, No. 2, March 1988, P. 190-197.
  - T. Ogata, T. Yuri, M. Saito and Y. Hirayama, "Fatigue Properties of Weld Joints of Stainless Steels and Aluminum Alloy at Cryogenic Temperature", Advances in Cryogenic Engineering (Materials), Vol. 46, Kluwer Academic/Plenum Publishers, 2000.
- Deposition Transcript of Anand David Kasbekar, Ph.D., 12-13-2019
- Report of Anand David Kasbekar, Ph.D. dated October 15, 2019 (Filed Under Seal)
- Deposition of Anand Kasbekar, Ph.D. dated November 25, 2020
- Rebuttal Report of Franklin Miller dated December 4, 2020
- Finite element analysis provided in Appendix 1 of this report



**Unknown Pls V. Chart, Inc., et al.**  
ESI Project No: 70497H

## Discussion

ESi has reviewed the expert report of Dr. Anand Kasbekar, dated 6-November-2020 and his deposition taken on 25-November-2020. Dr. Kasbekar makes various observations and claims regarding the crack in the fill line fitting-to-inner shell weld. Dr. Kasbekar makes several erroneous observations and conclusions that are discussed herein.

[View Details](#)

© 2013 Pearson Education, Inc.

[REDACTED]

**T**he following is a list of the most frequently asked questions about the new system. It is not intended to be all-inclusive, but it does cover the most common concerns.

---

---

---

---

---

---

---

---

---

---

---

---



**Unknown Pls V. Chart, Inc., et al.**  
ESI Project No: 70497H

## The 125 µm



**Unknown Pls V. Chart, Inc., et al.**  
ESI Project No: 70497H

<sup>1</sup> ASM Handbook, Volume 11, Failure Analysis and Prevention, 2002, P. 1069.



**Unknown Pls V. Chart, Inc., et al.**  
ESi Project No: 70497H

during its lifetime (2,200 cycles or less). As shown in the following graphs<sup>2,3</sup>, at liquid nitrogen temperature [REDACTED]

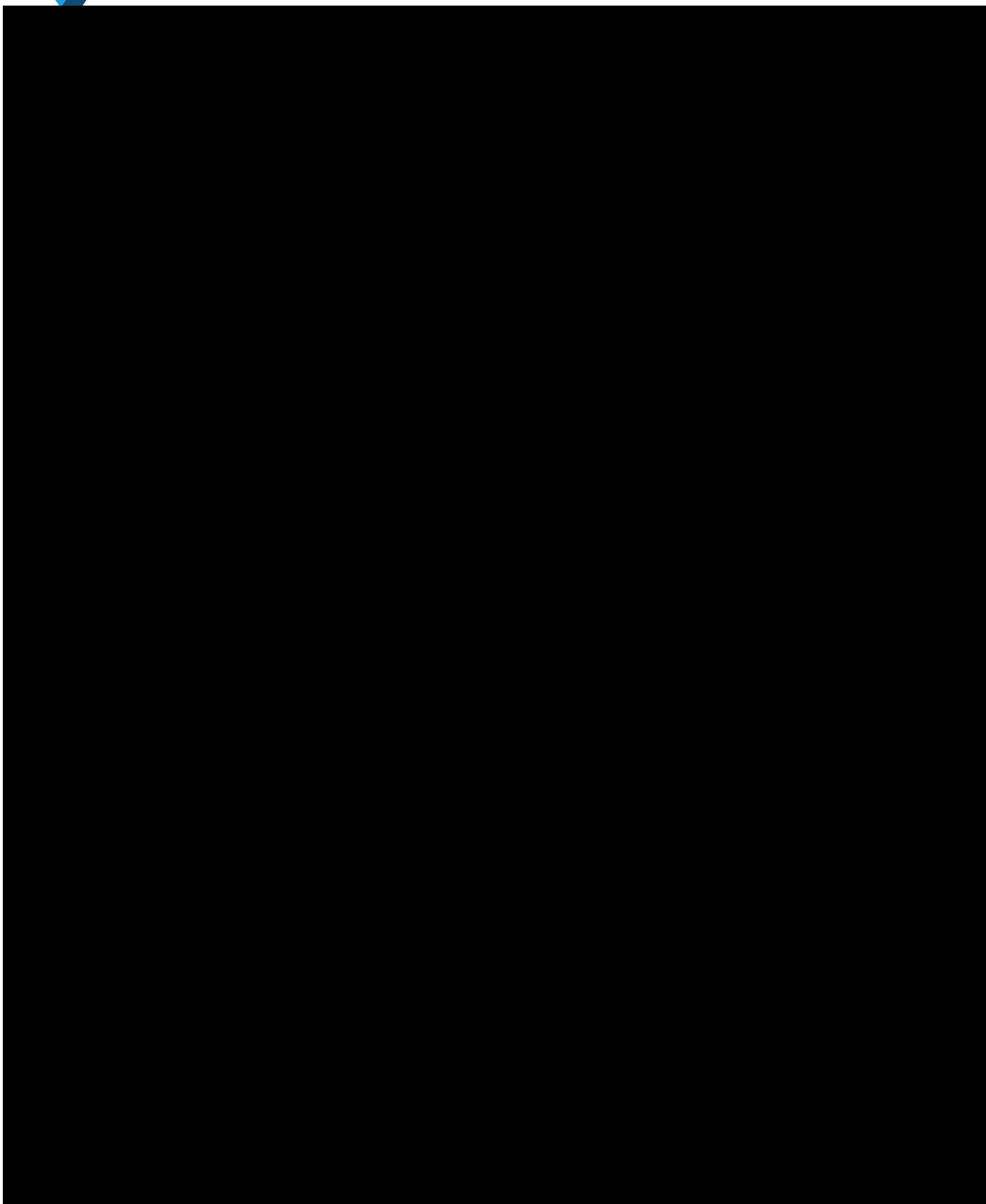
100

---

---



Unknown Pls V. Chart, Inc., et al.  
ESI Project No: 70497H





ESi reserves the right to supplement or amend these findings and conclusions if additional information becomes available or based upon additional work or analysis in this matter.

<<< End of Report Text >>>

## **Appendix 1**

---

### **Finite Element Analysis of Dr. Jay Sohn**

**Submitted by:**

A handwritten signature in black ink, appearing to read "Sangjoon Sohn".

---

**Jay Sohn, Ph.D.**  
**Senior Consultant**

---

December 4, 2020

---

Date



ESI was retained to conduct a cyclic stress/strain analysis of the CHART cryogenic tank subjected to tubing contraction due to the thermal differential when the tank is filled with liquid nitrogen and then returned to a normal state after filling is complete. For this purpose, a finite element model of the cryogenic tank was constructed using Abaqus™ FEA software. The modeling of the cryogenic tank was partially based on the x-ray scanned measurements<sup>1</sup> of the subject tank, in addition to the available part drawings<sup>2</sup> of the subject cryogenic tank.

The three-dimensional linear elastic finite element model consisted of a 90-degree quadrant section of the cryogenic tank, utilizing the symmetric nature of the cylindrical cross-section geometry of the tank. Figure 1 depicts the finite element model. As seen in Figure 1, the bottom of the tank has been truncated for computational efficiency. Two rigid surfaces were positioned in the FEA model, one on the top and one on the bottom. The bottom rigid surface represented the floor foundation, which the tank rested upon. The top rigid surface was placed to prevent dynamic rigid body motion during the computation. All the interfacing surfaces among the parts of the tank assembly were considered perfectly bonded, simulating welding. Figure 2 illustrates the joining of the tubing to the outer top head. The welded joint at this interface was simulated with a tie constraint in Abaqus, which bonds the two adjoining nodes of the sections. Weld reinforcement face of the elbow to the ID of the inner wall was simplified with a raised face. An overview of the raised face weld reinforcement of the inner wall is shown in Figure 3. A cross-section of the tubing-elbow-inner wall-weld reinforcement raised face is depicted in Figure 4 with dimensions.

A total of 351,619 three-dimensional solid elements were used in modeling the cryogenic tank. Representative images of the mesh used in the analysis are depicted in Figure 5. Sections that were uniform in geometry enabling a simplified meshing scheme were modeled using hexahedron elements (a 20-node quadratic with reduced integration). Sections where meshing with hexahedron elements was impractical were meshed with tetrahedron elements (a 10-node quadratic).

Since linear elastic assumption was used in modeling the cryogenic tank, elastic modulus and Poisson's ratio were required, which are listed in Table 1. In Table 1, the thermal expansion coefficient that was used in the analysis is provided, as well. The interaction between the rigid surfaces and the cryogenic tank was modeled with frictionless contact.

The analysis consisted of two steps. In the first step, a pressure (equivalent to the atmospheric pressure) was applied to the interior and the exterior surfaces of the tank, while the interstitial space between the tank inner sheet and the tank outer sheet remained unpressurized. This condition simulated the vacuum space that exists in between the two shells. In the second step of the analysis, the fill line tube was thermally strained while the atmospheric pressure was maintained on the surfaces that were pressurized in the first step. The approximately 26 inches of the tubing (tubing A, in Figure 2), which represented the span between the welded section of the outer top head and the welded section of the tubing to the elbow, had a thermal strain

---

<sup>1</sup> ESI work product consisting of scanned images of the tubing-elbow-inner wall-weld reinforcement section.

<sup>2</sup> Bates Number: CHART000063, CHART000091, CHART000096, CHART000104, CHART000107, CHART000108, CHART000115.



applied that was equivalent to a contraction of 0.023 inches.<sup>3</sup> This magnitude of thermal contraction was calculated by Dr. Franklin Miller from his thermal analysis.<sup>4</sup>

The top and bottom rigid surfaces were constrained all 6 degrees of freedom (three translational and three rotational), thus providing resistance to any rigid body dynamic motion. The two 90-degree cross-sections of the tank were constrained with symmetry boundary conditions (x-symmetry and z-symmetry). A pressure of 14.7 psi, which is equivalent to 1 atmospheric pressure, was applied to the interior and the exterior surfaces of the tank, including the top and bottom of the tank. This pressure was maintained in the second step. The thermal strain from the 0.023 inches of tubing contraction was simulated by thermal expansion/contraction in the manner described in the preceding paragraph. The boundary condition and the loading condition is illustrated in Figures 6 and 7, respectively.

As based on the observation of the existing data on the fill cycle of the liquid nitrogen<sup>5</sup>, the focus was on assessing the low cycle fatigue of the tank assembly with the main interest in the weldment of the elbow to the inner wall (presumably, where a crack was observed<sup>6</sup>). Based on these observations, two possible fatigue hotspot locations were selected:

- Weld reinforcement raised face area on the inner wall
- Weld root area of the elbow to the inner wall

These locations are visually presented in Figure 8. Due to the fact low cycle fatigue was to be investigated, the total accumulated strain was of importance and the FEA result is assessed with maximum principal strain. The cyclic nature of the load was reciprocating between: Step 1) liquid nitrogen empty normal state at atmospheric pressure load and Step 2) liquid nitrogen filling state at atmospheric pressure load (excluding the vacuum space). Thus, the total strain range,  $\Delta\varepsilon_{\text{tot}}$ , can be defined as  $\Delta\varepsilon_{\text{tot}} = \varepsilon_2 - \varepsilon_1$ .





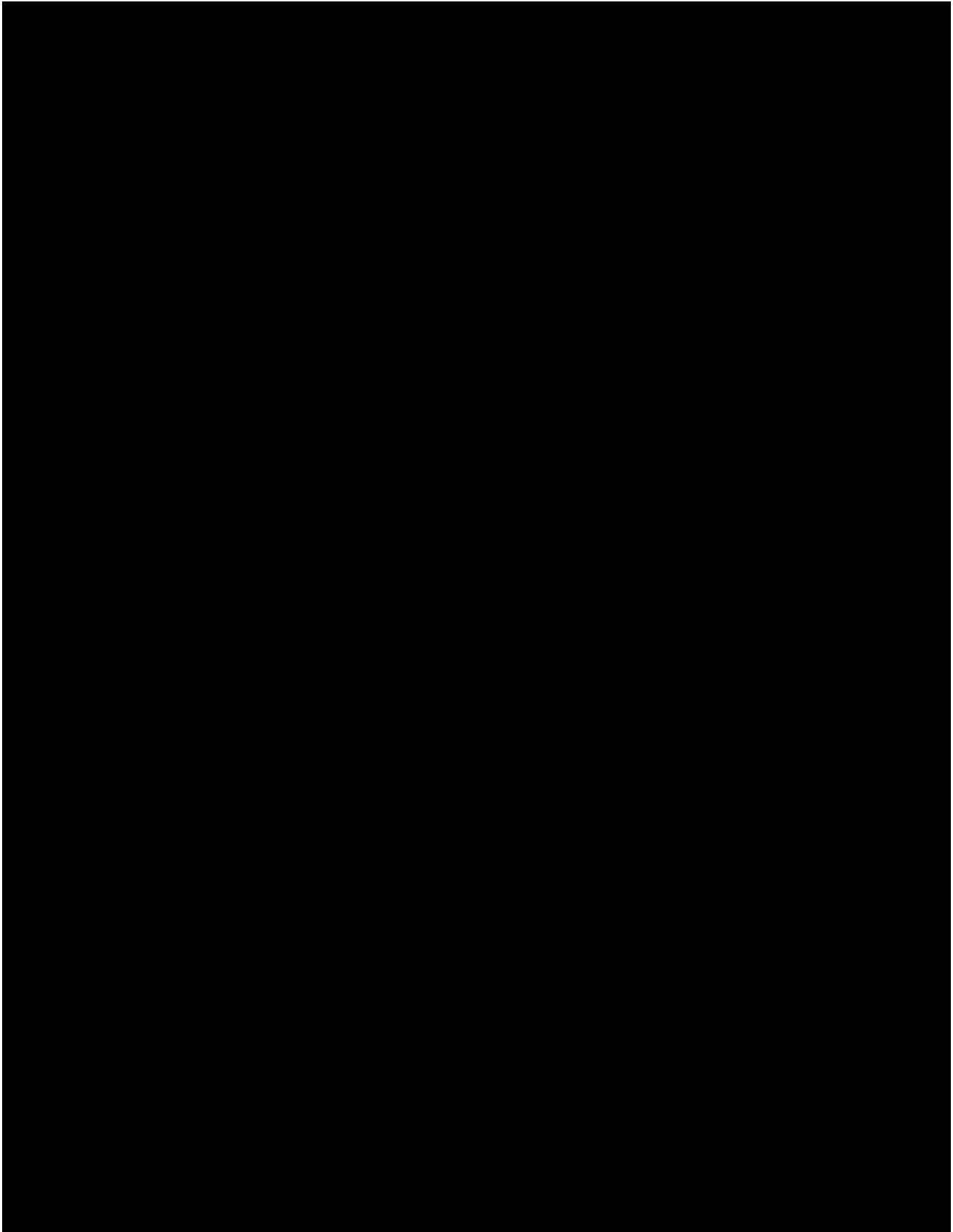
**Unknown Pls V. Chart, Inc., et al.**  
ESI Project No: 70497H

Term	Percentage (%)
GDP	95
Inflation	95
Interest rates	95
Central bank	95
Monetary policy	95
Quantitative easing	95
Institutional investors	95
Fintech	95
Algorithmic trading	95
Blockchain	95
Smart contracts	95
RegTech	95
FinTech	95
Robo-advisors	95
Digital currencies	95
Central bank digital currencies	95
Stablecoins	40



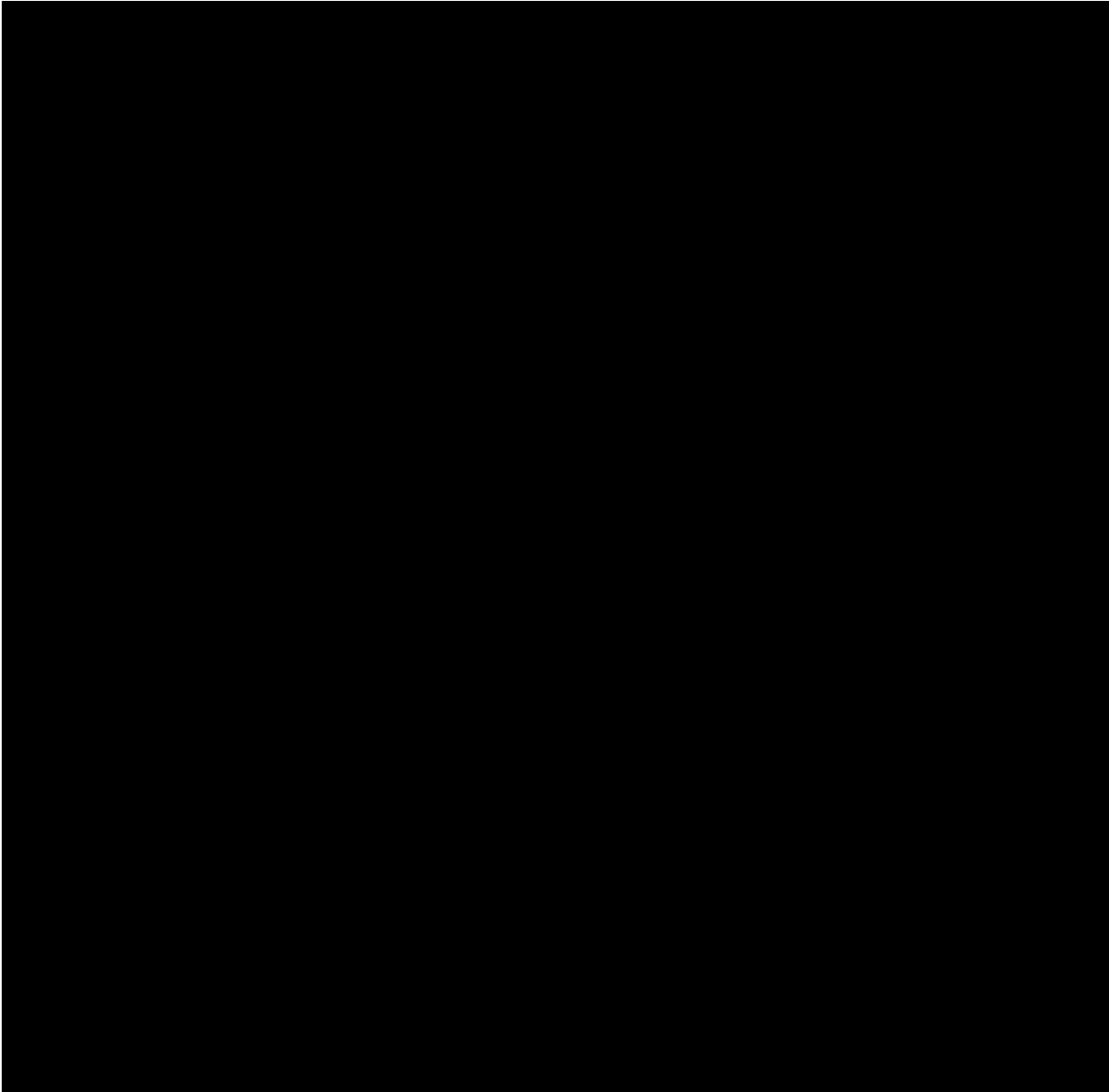


Unknown Pls V. Chart, Inc., et al.  
ESI Project No: 70497H



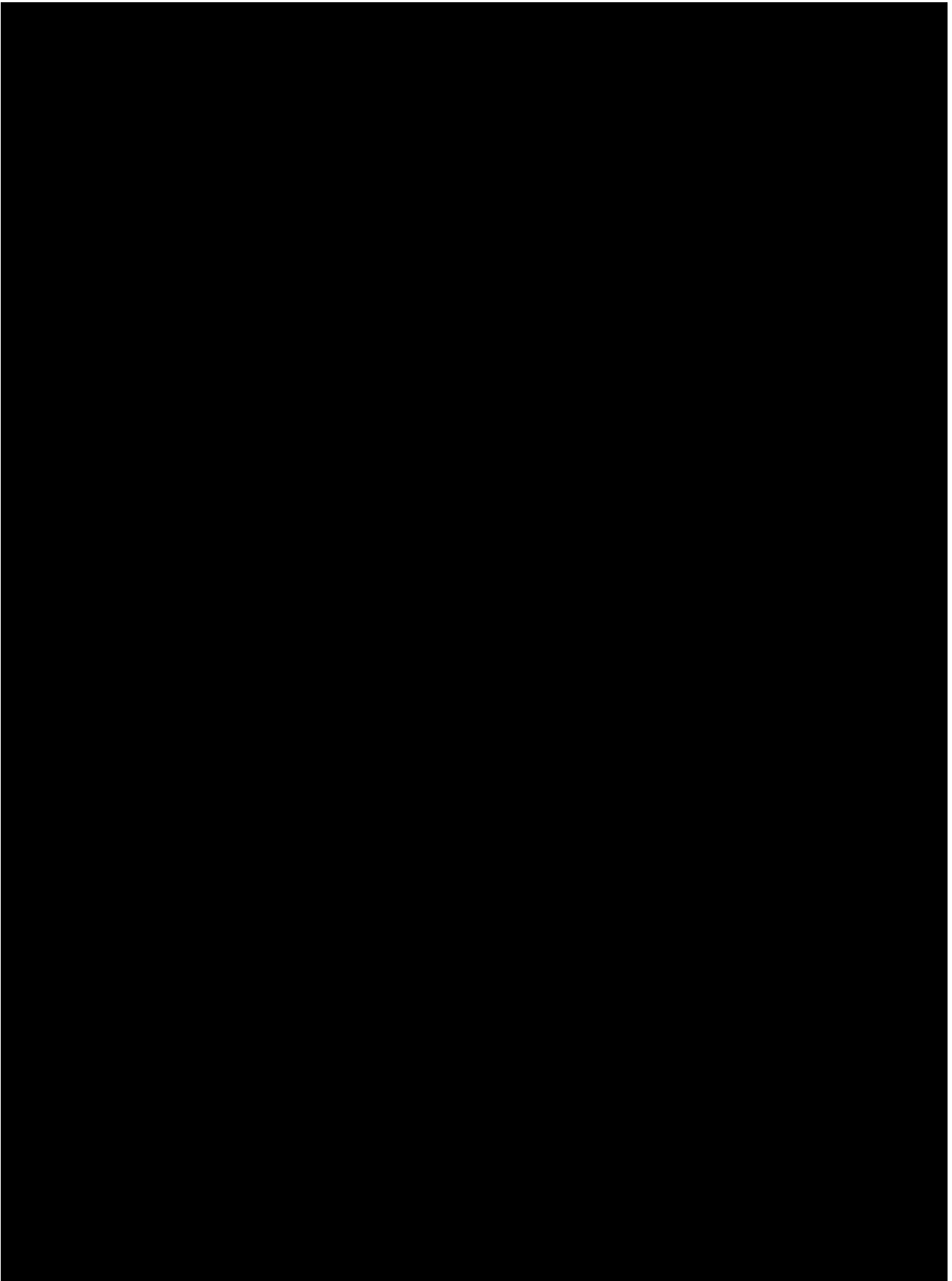


Unknown Pls V. Chart, Inc., et al.  
ESI Project No: 70497H



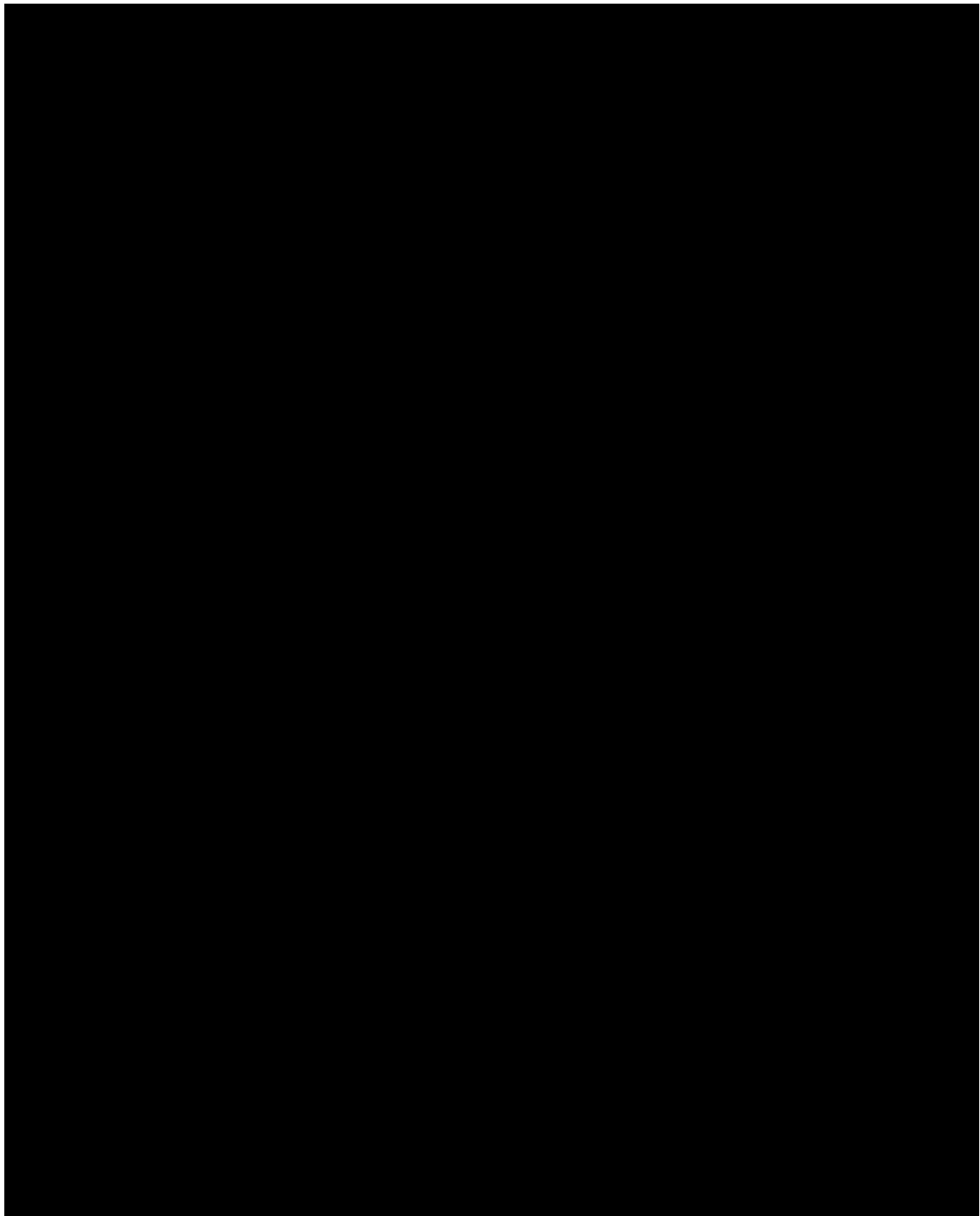


Unknown Pls V. Chart, Inc., et al.  
ESI Project No: 70497H



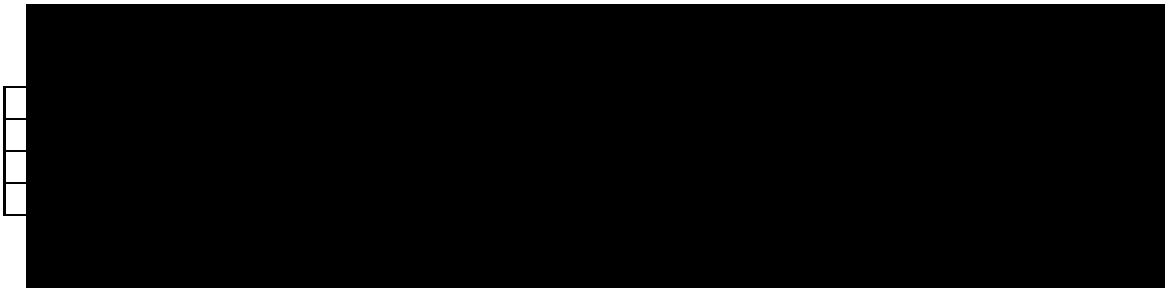


Unknown Pls V. Chart, Inc., et al.  
ESI Project No: 70497H



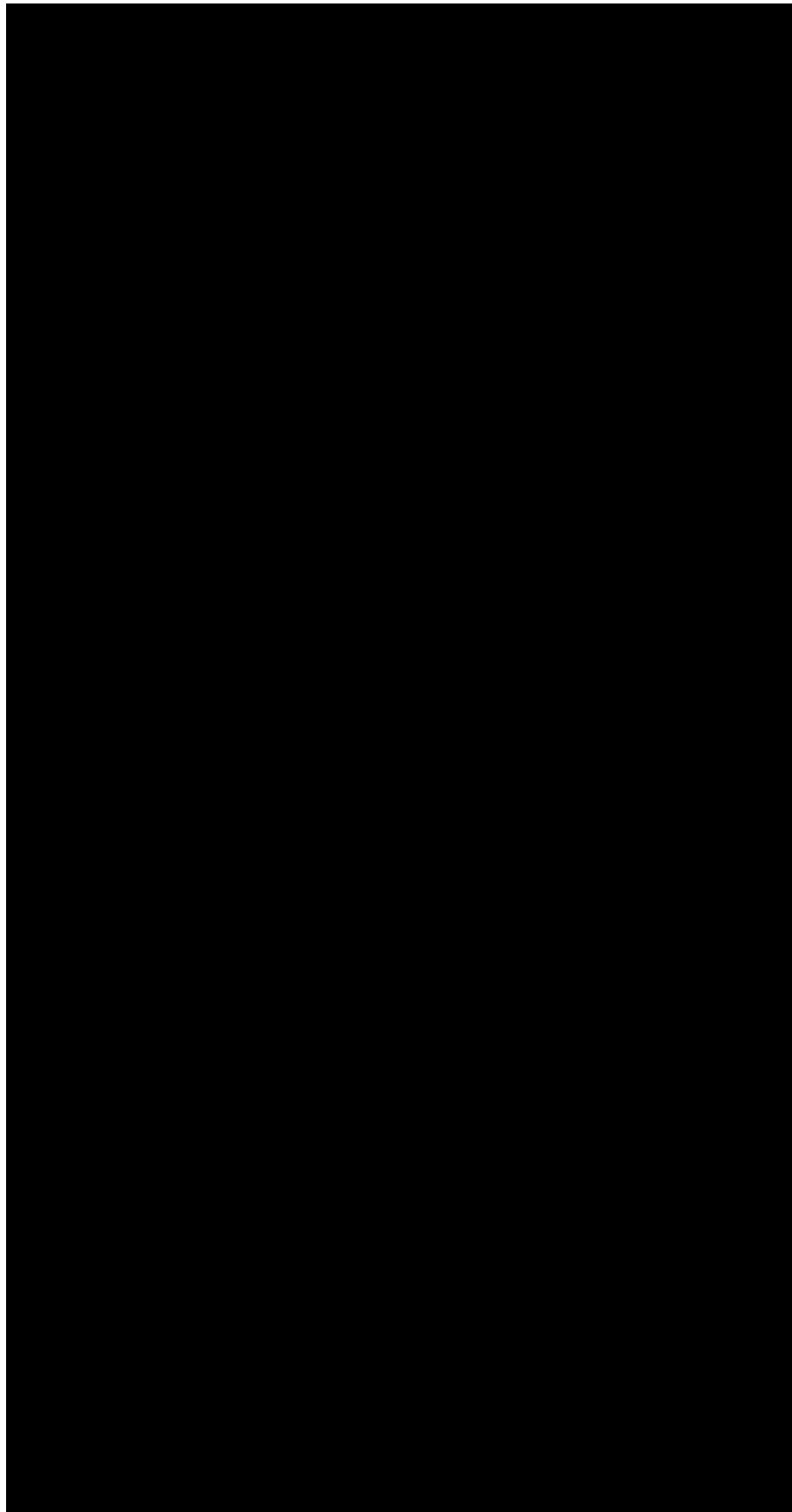


Unknown Pls V. Chart, Inc., et al.  
ESI Project No: 70497H





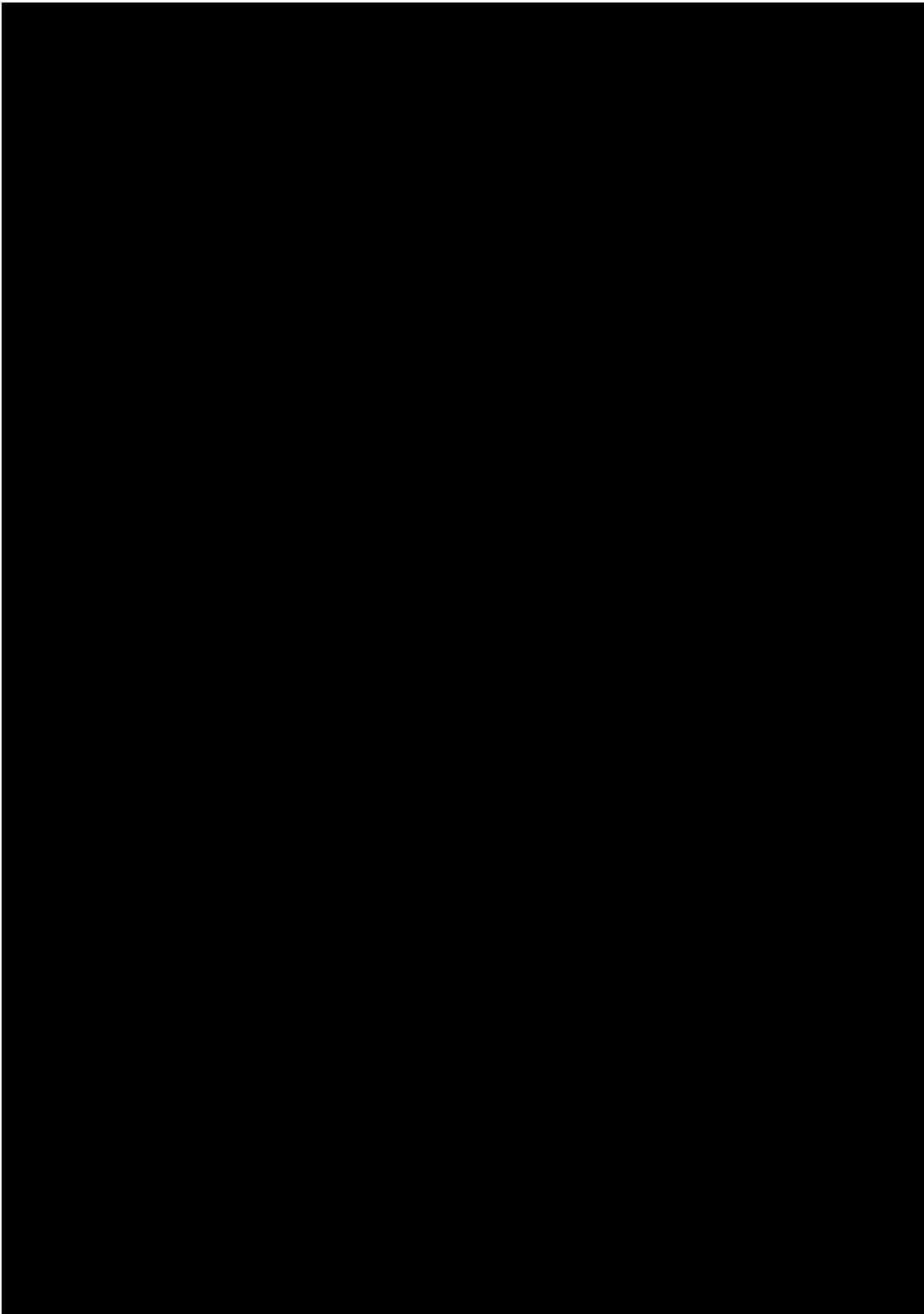
Unknown Pls V. Chart, Inc., et al.  
ESI Project No: 70497H



**Fig**



Unknown Pls V. Chart, Inc., et al.  
ESI Project No: 70497H





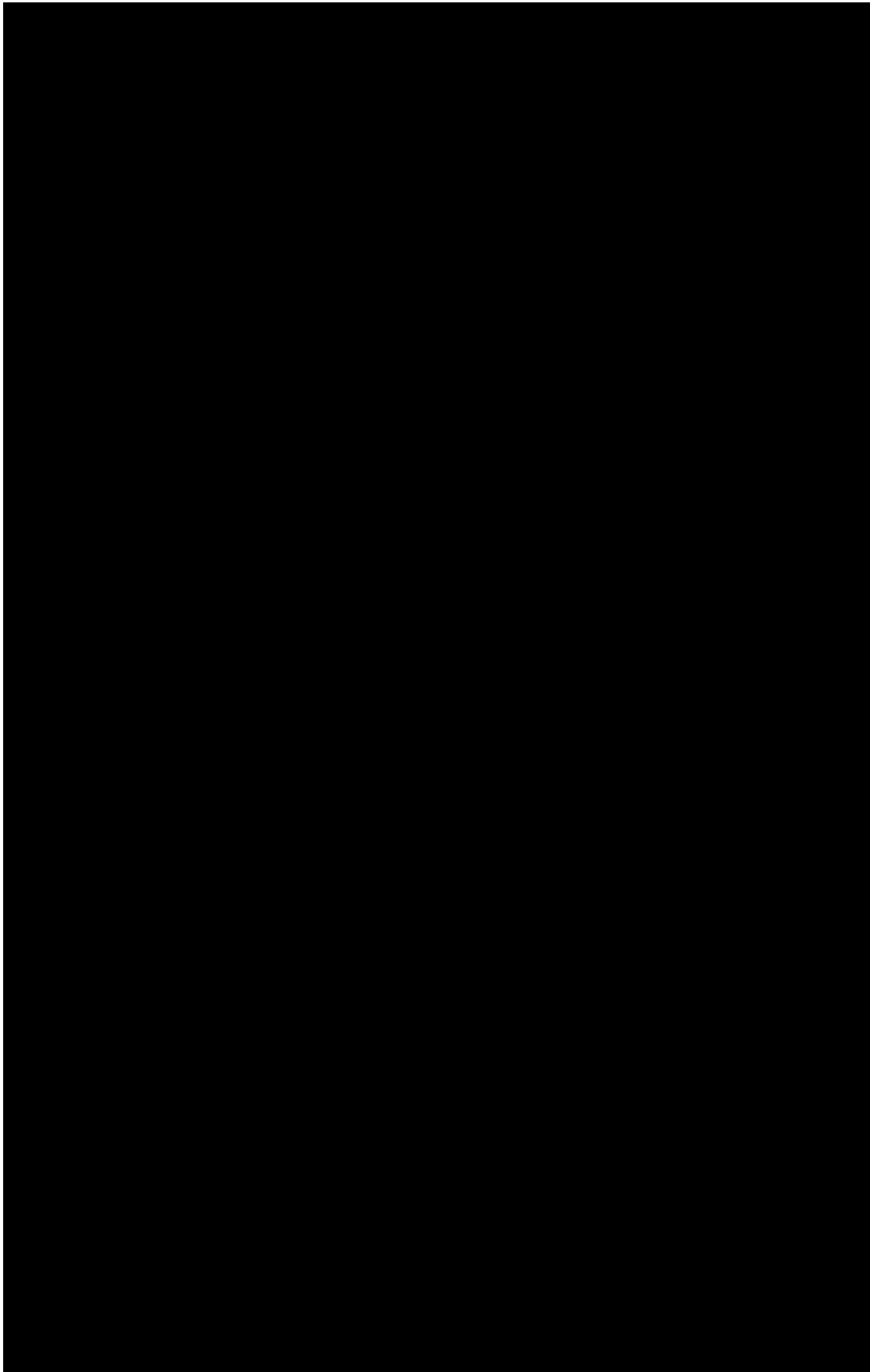
Unknown Pls V. Chart, Inc., et al.  
ESI Project No: 70497H

P  
Weld

A red rectangular box with a thin black border, containing the text 'P Weld'. It is positioned to the left of a large black rectangular area that covers most of the page content.

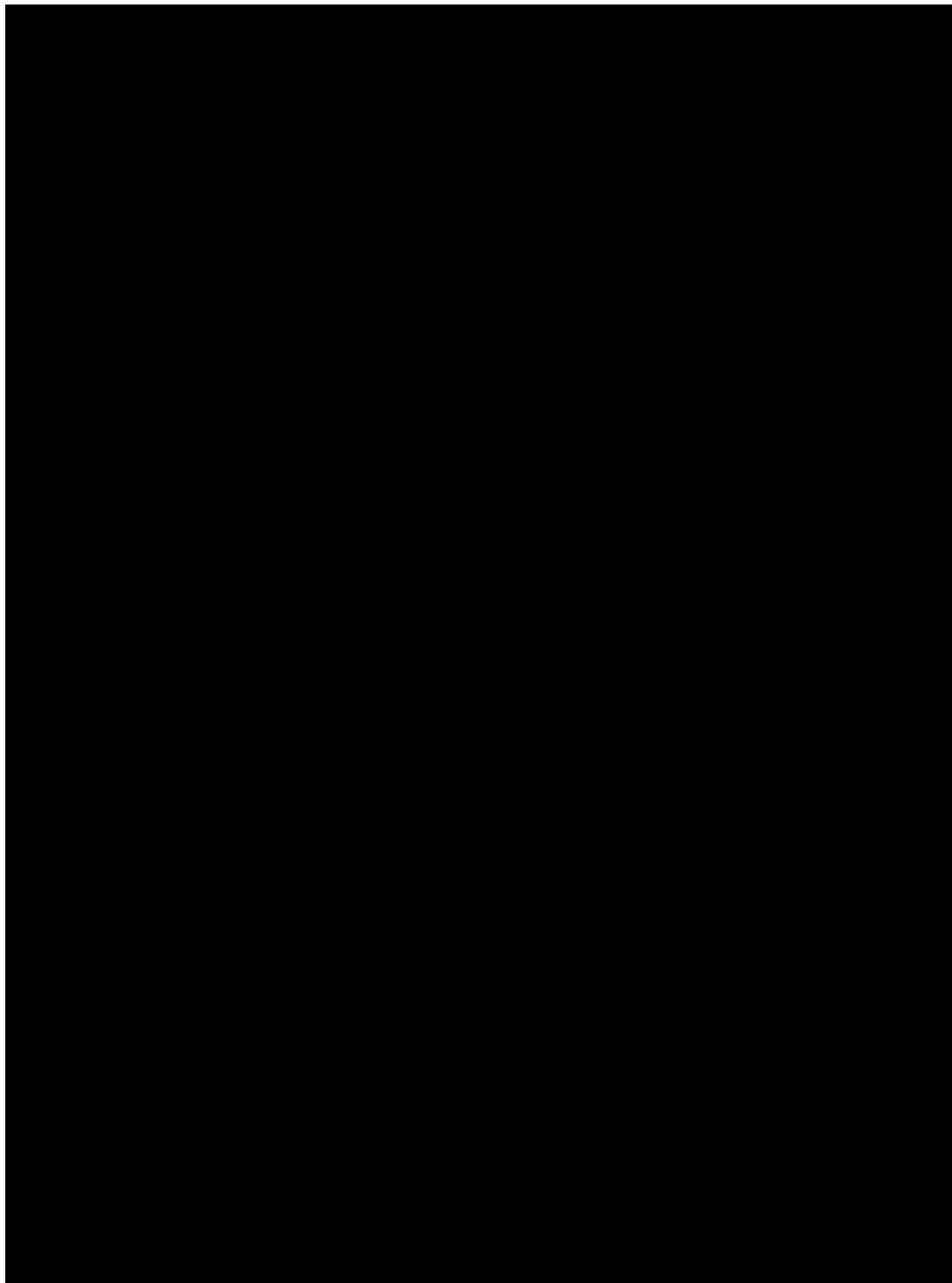


Unknown Pls V. Chart, Inc., et al.  
ESI Project No: 70497H



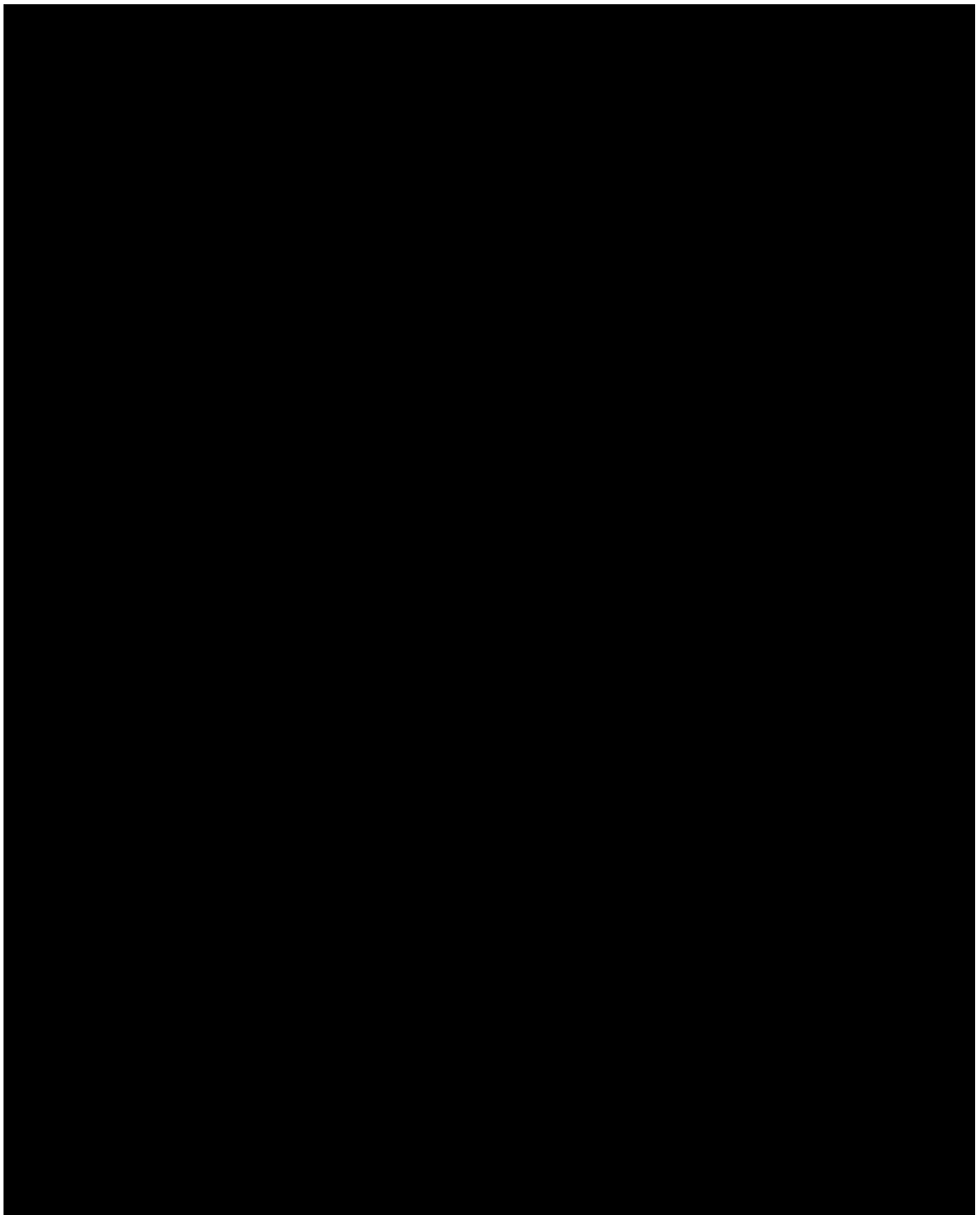


Unknown Pls V. Chart, Inc., et al.  
ESI Project No: 70497H



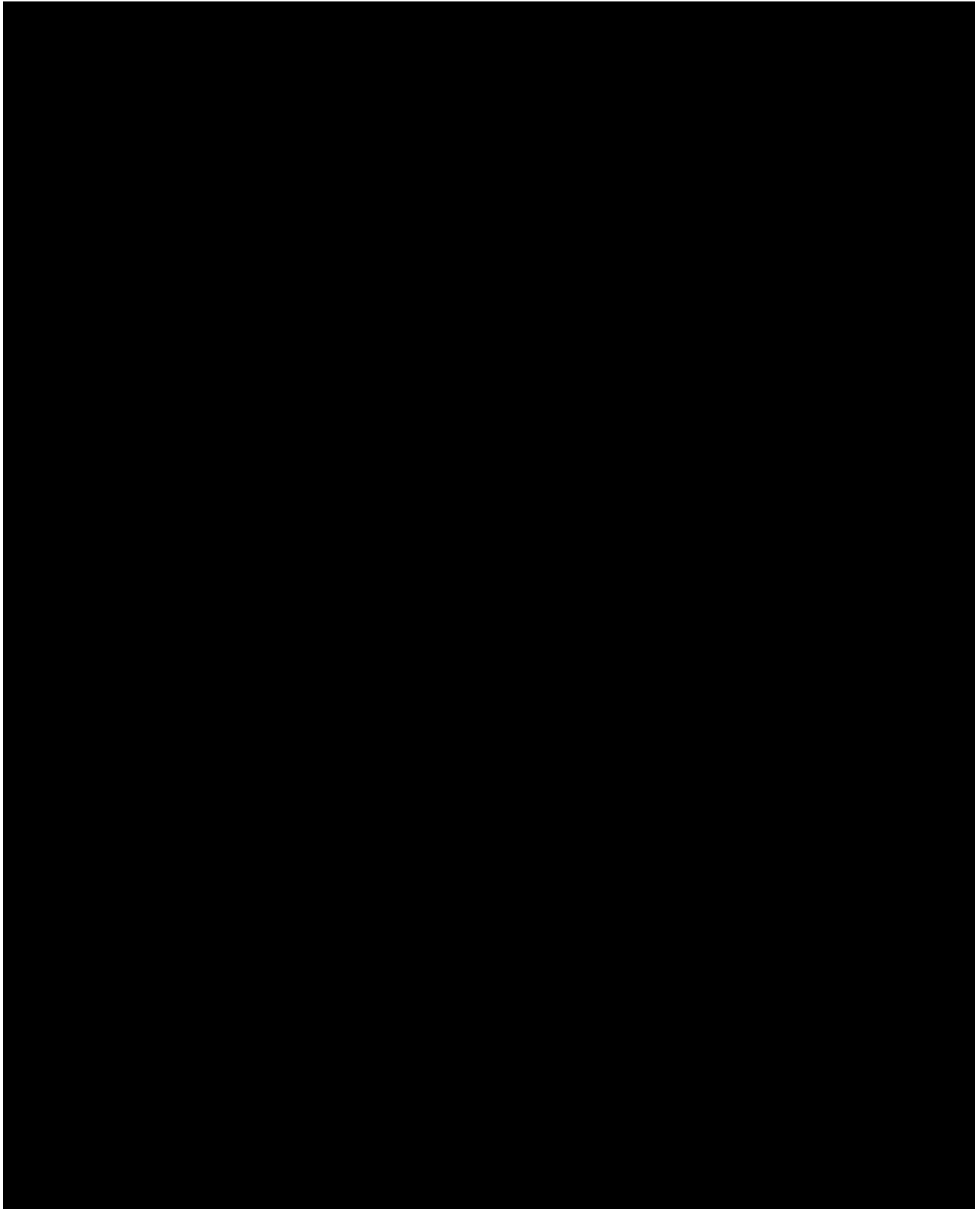


Unknown Pls V. Chart, Inc., et al.  
ESI Project No: 70497H



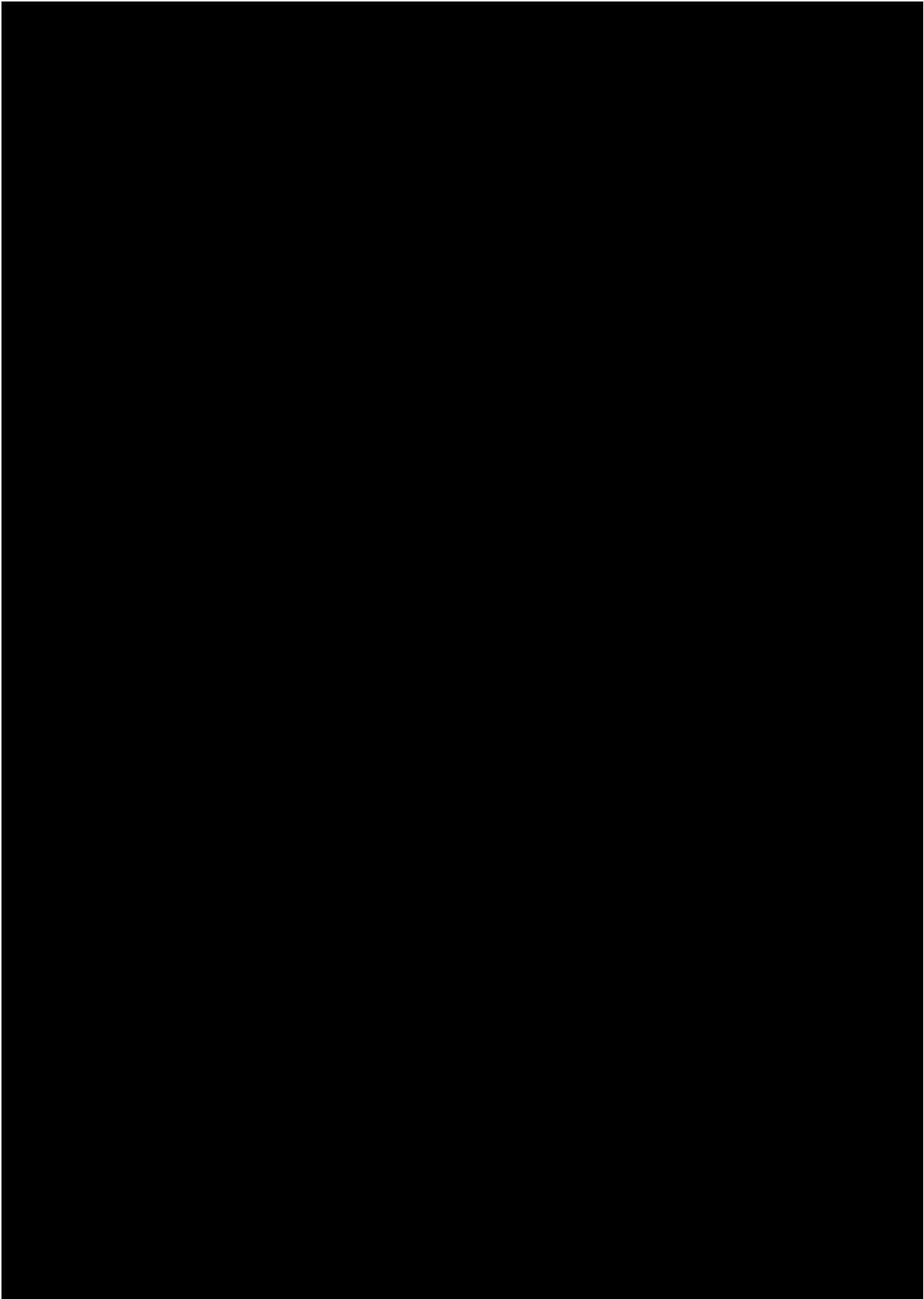


Unknown Pls V. Chart, Inc., et al.  
ESI Project No: 70497H



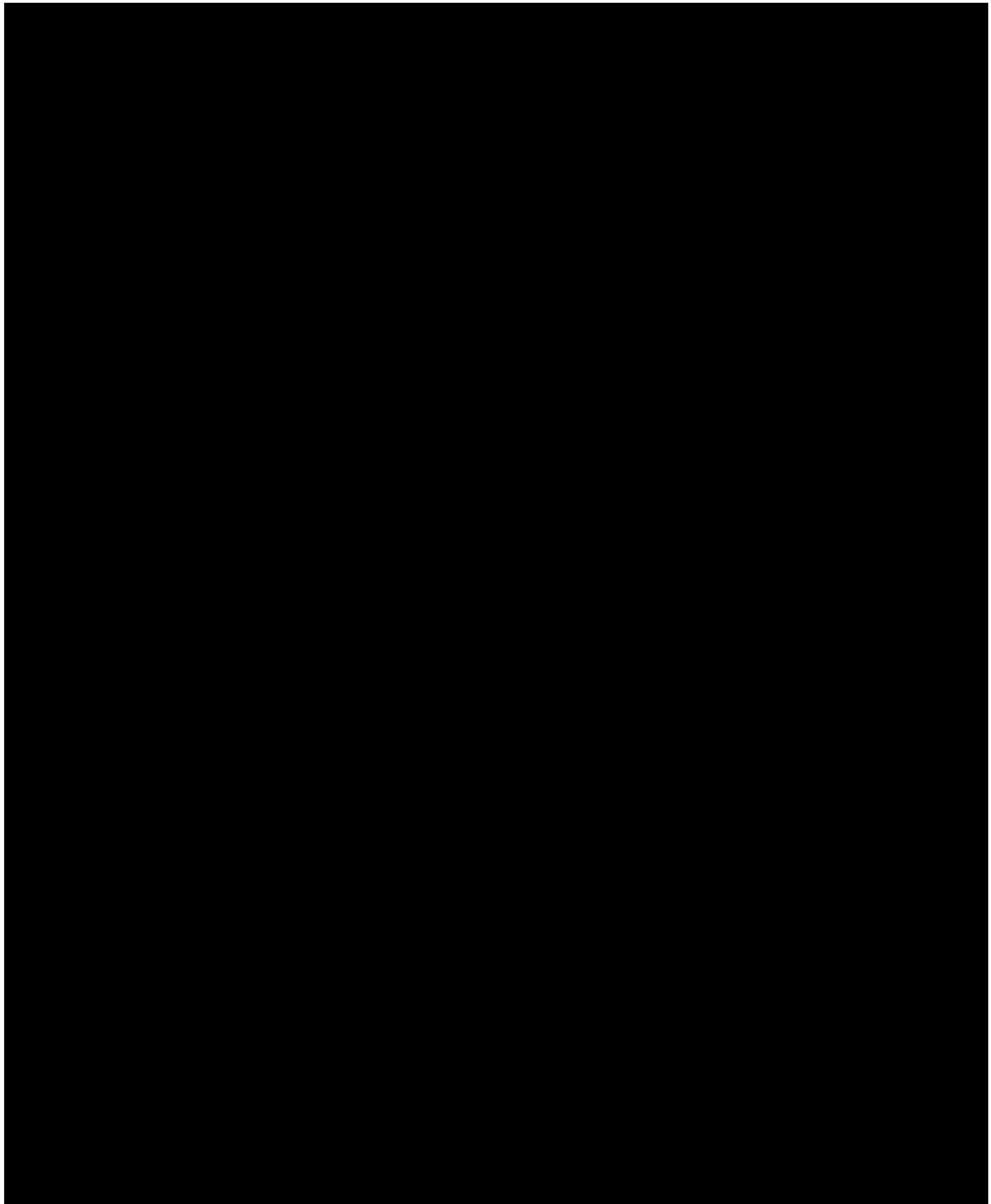


Unknown Pls V. Chart, Inc., et al.  
ESI Project No: 70497H





Unknown Pls V. Chart, Inc., et al.  
ESI Project No: 70497H





Unknown Pls V. Chart, Inc., et al.  
ESI Project No: 70497H

